Molecular mechanisms in the pyrolysis of unsaturated chlorinated hydrocarbons

Grant J. McIntosh* and Douglas K. Russell

Received (in Montpellier, France) 20th May 2008, Accepted 23rd July 2008
First published as an Advance Article on the web 10th September 2008
DOI: 10.1039/b808495e

Laser-induced pyrolysis of small chlorinated hydrocarbons at temperatures where radical processes are likely to be unimportant has provided clear evidence for direct low-energy molecular reactions between acetylenes and chlorinated acetylenes or ethylenes. High-level *ab initio* calculations of possible pathways have shown that these reactions proceed *via* two routes. Direct bimolecular reaction accompanied by HCl elimination leads to diacetylenes or vinylacetylenes, respectively, while carbene molecular adducts, followed by Cl or H migrations to yield three- or four-membered rings and ring-opening, lead to vinylacetylenes or butadienes, respectively. Analogues of these processes are likely to be central to the growth of larger molecules in such systems.

Introduction

The gas-phase formation of molecules containing several carbon atoms from smaller precursors has been of both practical and fundamental interest for many years. Many simple hydrocarbons lead to complex systems such as aromatic and polyaromatic hydrocarbons (PAH's) and even fullerenes on pyrolysis, combustion or photolysis. Despite extensive experimental and theoretical study, the detailed mode of formation of these systems is still controversial.

In particular, the mechanism of the thermal reaction of acetylene has been a contentious issue for some time. Vinylacetylene is known to be the major product in the lower temperature ranges of acetylene pyrolysis;[1–3] benzene is also formed in high yield.[1,3] To a lesser extent, diacetylene,[4] 1,3-butadiene,[5] polyynes,[6] PAH's,[7] and under certain conditions and with co-pyrolysis materials, fullerenes[8–10] have also been observed. A number of radical-initiated routes have been proposed, given the traditional indications of induction periods[1] and reaction inhibition in the presence of radical scavengers such as nitric oxide.[11–13] Disproportionation of two acetylene molecules to form vinyl and ethynyl radicals was proposed over 30 years ago by Back;[14] data compiled later by Durán *et al.*[15] provided two estimates for the enthalpy of this reaction at 370.7 and 345.6 kJ mol^{-1}. Minkoff proposed the partial rupture of an acetylenic triple bond and rapid reaction of the resulting biradical;[16] recent experimental[17] and computational[18] investigations of the energy required to excite this bent $\tilde{a}\,^3B_2$ state, relative to the linear $X\,^1\Sigma_g^+$ ground state, found 345.9 and 369.8 ± 2.8 kJ mol^{-1}, respectively. Although the estimates for these two proposed reactions are in agreement with each other, both are significantly higher than the experimental activation energy of the initiation reaction, recently estimated[1] to be approximately 260 kJ mol^{-1}. A bimolecular initiation reaction between two C_2H_2 molecules, forming C_4H_3 and H atoms[2,6,19] has also received attention, with the enthalpy of reaction being estimated at 192 kJ mol^{-1}.

Durán *et al.*, however, argued that radical routes below 1300 K lead to acetylene decomposition rates much slower than observed, and furthermore predict benzene (rather than vinylacetylene) as the major product.[15] They instead proposed decomposition *via* vinylidene, $H_2C{=}C{:}$, which has an activation barrier to formation from acetylene of 184.3 kJ mol^{-1}, as calculated at the QCISD(T)/6-311 + G(*d*,*p*)//MP2/6-31 G(*d*,*p*) level.[20] The involvement of this species was further explored by Ghibaudi and Colussi, who suggest that methylenecyclopropene is a likely short-lived intermediate in the conversion of acetylene to vinylacetylene *via* the vinylidene route.[21] This mechanism was eventually reconciled with early observations such as autoacceleration and inhibition by radical scavengers, which seemingly point to radical processes, by Kiefer and von Drasek.[22,23]

Comparatively little mechanistic work into molecular growth pathways involving chlorinated ethylenes and acetylenes has been undertaken; what has is based largely around the chemistry of trichloroethylene. Taylor *et al.*[24] undertook modeling experiments of the high-temperature pyrolysis of C_2HCl_3, and also observed C_4Cl_4 to be the major C_4 product. The authors concluded that C–Cl bond rupture in C_2HCl_3 was the dominant initiation step; liberated Cl atoms abstracted H atoms from C_2HCl_3, providing a source of C_2Cl_3. This either decomposed to C_2Cl_2 + Cl, reacted with Cl_2 to form C_2Cl_4 + Cl, or with C_2HCl_3, C_2Cl_2 and C_2Cl_4 yielding (after loss of a further Cl) C_4HCl_5, C_4Cl_4, and C_4Cl_6, respectively.

Earl and Titus[25] proposed an alternative reaction mechanism, proceeding *via*

$$ClC{\equiv}CCl \rightarrow ClC{\equiv}C^{\bullet} + Cl^{\bullet}, \quad (1)$$

$$ClC{\equiv}C^{\bullet} + ClC{\equiv}CCl \rightarrow ClC{\equiv}C{-}CCl{=}C(Cl)^{\bullet} \quad (2)$$

These authors proposed that Cl atom addition to, or Cl abstraction by, C_4Cl_3 provides the major route to C_4Cl_4. This

Department of Chemistry, University of Auckland, Private Bag, Auckland, 92019, New Zealand. E-mail: d.russell@auckland.ac.nz; Fax: 0064 9 373 7422; Tel: 0064 9 373 7599 ext 88303

mechanism has been adopted by Drijvers *et al.*[26] in the sonolysis of trichloroethylene in aqueous solution, which induces largely pyrolytic reactions inside the cavities of rapidly collapsing bubbles. Product yields were similar to those observed in previous C_2HCl_3 pyrolysis studies,[24,25] however, additional products C_2HCl and C_4HCl_3 were also detected. Formation of C_4HCl_3 was rationalized by employing reaction (1) followed by reaction (3):

$$ClC{\equiv}C^{\bullet} + HC{\equiv}CCl \rightarrow HC{\equiv}C{-}CCl{=}C(Cl)^{\bullet}, \quad (3)$$

again followed by a Cl addition or abstraction step.

Other possible mechanisms in chlorinated systems may be drawn from analogous processes in the parent hydrocarbons. One such is based on vinyl radicals; this is an attractive starting point due to observed reaction inhibition by radical scavengers like nitric oxide[11–13] and the determination of an induction period[1,12,27] in product formation during C_2H_2 pyrolysis. However, this pathway has been dismissed by Xu and Pacey,[1] since the energy of the initiation step that they measured, 261 ± 11 kJ mol^{-1}, is much lower than the calculated energy of the disproportionation reaction (370 kJ mol^{-1}, as provided by Duran *et al.*[15]). Furthermore, when extended to chlorinated systems, the C_2H radical would be expected to form C_4H_2-based products.

Another extensively discussed route involves the formation of vinylidenes, :C=CXY, which may insert into the C–H bond of a second acetylene molecule.[15,22] This is particularly attractive in light of the low (194.8, 188.3, and 215.9 kJ mol^{-1} for C_2H_2, C_2HCl, and C_2Cl_2, respectively[20,28]) activation energies for the most favorable acetylene to vinylidene rearrangement for each species. The recently determined longer than anticipated lifetime of :C=CH_2[29,30] supports the involvement of :C=CH_2 in molecular growth; however, chloro- and dichlorovinylidene are expected to revert back to the more stable acetylenic structure much faster than any other reaction (for example, HCl loss) to be significantly involved in growth processes.

We have recently initiated a series of investigations of the pyrolysis of simple chlorinated hydrocarbons such as dichloromethane and chlorinated ethylenes using the technique of laser-powered homogeneous pyrolysis, with the ultimate aim of producing fullerene-related systems. In the course of this study, we have uncovered experimental and computational evidence of mechanisms which may have a substantial bearing on the parent hydrocarbon systems. In the present work, we report novel molecular carbon-chain growth mechanisms involving chlorinated acetylenes and ethylenes.

Experimental

Chemicals

All chlorocarbons and other compounds used were of analytical grade quality and obtained commercially. These and SF_6 (BOC) were purified before use by repeated freeze–pump–thaw cycles. Materials were handled on Pyrex vacuum lines fitted with greaseless taps; before use, the line was preconditioned by exposure to the vapor under study and re-evacuation. Precursor and product identification and analysis (FT-IR spectroscopy and GC-MS) were accomplished using commercial instrumentation in conjunction with comparison with data from authentic samples (where available).

Infrared laser-powered homogeneous pyrolysis

All static cell pyrolyses utilized the IR LPHP technique. Since this method has been described in detail elsewhere, only a brief description is given here.[31–34] Pyrolysis is performed in a cylindrical Pyrex cell (length 100 mm, diameter 38 mm) fitted with ZnSe windows. Although ZnSe is opaque to infrared radiation below 500 cm^{-1}, it has several distinct advantages over cheaper materials, such as NaCl. ZnSe is strong and thermally stable, and non-hygroscopic. Most significantly, ZnSe is highly transparent to the CO_2 laser radiation. The pyrolysis cell is filled with between 10 and 20 Torr (1 Torr = 133.3 Pa) of the vapor under study and approximately 8 Torr of SF_6. The contents of the cell are then exposed to the output of a free running CW CO_2 laser operating at 10.6 μm. The laser power level (which determines the temperature) is generally set close to the threshold required for measurable decomposition of the target compound, with an exposure time sufficient to provide an analyzable yield of products, typically a few% decomposition. As shown elsewhere,[31,34] SF_6 strongly absorbs the laser radiation, which is then rapidly converted to heat *via* efficient inter-molecular and intra-molecular relaxation. The low thermal conductivity of SF_6 ensures that a strongly non-uniform temperature profile is produced in which the centre of the cell may reach temperatures of the order of 1500 K while the cell wall remains at room temperature.[35]

IR LPHP has a number of well-documented advantages. The first of these is that pyrolysis is initiated directly in the gas phase, thereby eliminating the complications frequently introduced by competing surface reaction. Since surface–initiated reactions frequently involve free radicals, this factor enhances the role of molecular mechanisms. The second is that the primary products of pyrolysis are rapidly ejected into the cooler regions of the cell, inhibiting their further reaction. In favourable cases, these products may be accumulated for further investigation. One substantial disadvantage of IR LPHP is that the temperature of the pyrolysis is neither well defined nor easily determined, despite many experimental and theoretical approaches;[31,34] kinetic analysis and comparison with more conventional methods of pyrolysis are thus difficult. However, if a convenient non-interacting system of known activation energy is incorporated (either intentionally or adventitiously), one may use this as an internal benchmark. This approach was used extensively in the present work, as described in the Results section.

Under favourable circumstances, further mechanistic information may be obtained by the judicious use of additives. In particular, the formation of new products or a change in product distribution on co-pyrolysis with H_2 or D_2 is strong indirect evidence for the involvement of free radicals. This well-established method is based on the rapid reaction of many radicals with H_2: R + H_2 → RH + H.[36–38] We have exploited this to demonstrate, for example, the role played by thienyl radicals in the decomposition of thiophene.[39]

Analytical methods

The FTIR spectra presented in this work were recorded using a Digilab FTS-60 Fourier transform spectrometer at a resolution of 1 cm^{-1} and averaged over 10 scans per spectrum. Win-IR software was used to acquire and process spectral data. The sample compartment of the spectrometer, which contained the pyrolysis cell, was purged with N_2 to reduce/eliminate contributions of CO_2 and water from the ambient atmosphere. All spectra were collected against a background spectrum of an evacuated pyrolysis cell. FTIR spectra were used primarily to characterize small gaseous products such as acetylenes or HCl, where resolved vibration–rotation structure permits unambiguous identification even from a single band; in such cases, comparison with authentic samples (where available) was used for verification. The technique is less useful for larger molecules, in which similar vibrations often have almost identical bands, and it also lacks the sensitivity necessary for quantitative analysis. Absorptions were converted to molar concentrations using calculated absorption coefficients (see below for further details of calculations).

GC-MS analysis of gas samples was conducted using a Hewlett Packard 6890 series gas chromatograph interfaced with a Hewlett Packard 5793 Mass Selective Detector (MSD). Base pressure of the MSD was maintained at 1×10^{-5} Torr by a turbomolecular pump backed by a rotary pump. Gas samples were extracted from the pyrolysis cell, *via* the septum port, with a Hamilton 2.5 mL gas tight syringe fitted with a lockable valve. The contents of the cell were at relatively low pressure (20–30 Torr); typically, therefore, 2.5 mL of the gas sample were extracted, and after the syringe valve was engaged, the sample was compressed to 0.25 mL to achieve a pressure closer to atmospheric. A ''HP5-MS'' cross-linked phenyl methyl siloxane gum capillary column (i.d.: 0.25 mm, length: 29.2 m, film thickness: 0.25 μm) was employed as a multi-purpose column, while a ''GS GasPro'' column (i.d.: 0.32 μm, length: 30 m) was used for the detection and identification of low molecular weight species. Helium was used as the carrier gas in this GC-MS system. One drawback of the sample extraction method is that products of low volatility are not easily recovered from the pyrolysis cell, and therefore GC-MS must be used in conjunction with other methods for a complete analysis.

Computational methods

We have chosen density functional theory (DFT) methods throughout this work. All structures were optimized using the B3LYP functional[40,41] with the 6-31G* basis set since DFT methods have relatively low computational cost, especially with such small basis sets. Zero-point energies were also calculated at this level of theory, and were scaled[42] by 0.9806. Additional accuracy was afforded with DFT/B3LYP/6-31+G*//DFT/B3LYP/6-31G* level calculations. The use of this particular method for single-point energy calculations, and the use of DFT over MP2 methods, is justified in Table 1 where we have considered the activation energies for a number of computational methods, compared with either experimental or very high-level computational data, over a range of benchmark reactions similar to those considered in our study.

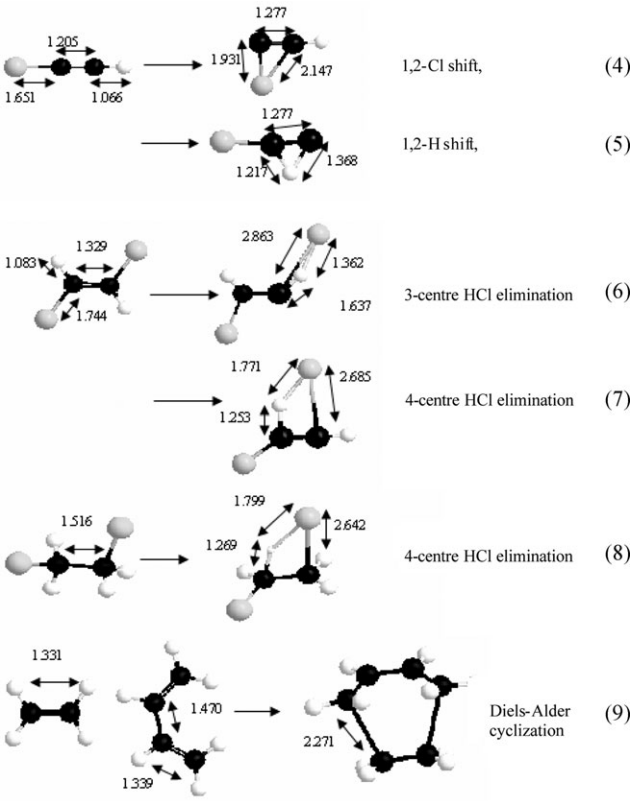

Fig. 1 Transition states for the benchmark reactions (4)–(9) of Table 1; bond lengths in Å from the DFT/B3LYP/6-31G* level of theory.

Columns in italics show the energy barriers of structures fully optimized at the quoted level of theory; all other columns represent single-point energy calculations based on these structures. All zero point energies are from the DFT/B3LYP/6-31G* level of theory. We see that our chosen method has both the smallest maximum and average deviations from the selected published data of all of the methods considered; furthermore, for the reactions considered (shown explicitly in Fig. 1), DFT methods out-perform MP2 calculations.

We have given DFT methods particular attention due to the expected importance of unimolecular HCl elimination processes[43] in small chlorinated hydrocarbons. As has been noted in numerous cases, DFT methods generally reproduce HCl elimination reactions better than other methods. Ferguson *et al.*[44] found the DFT/B3PW91/6-31G(d′,p′) method reproduced HCl eliminations from CH_3CH_2Cl, $CH_3CH_2CH_2Cl$, and $CF_3CH_2CH_2Cl$ to within 2 kJ mol^{-1}. In their analysis of 1,2-HF, HCl and ClF eliminations from CH_2FCH_2Cl, Rajamumar and Arunan[45] found that, while DFT methods underestimate HCl elimination barriers by approximately 20 kJ mol^{-1} for both the title compounds and chloroethane, they give very good agreement for 1,2-dichloroethane. Further, higher level methods (for example, CCSD and MP2) tended to overestimate barriers by approximately 20 to 30 and 40 to 50 kJ mol^{-1}, respectively.

We see, from Table 1, that DFT/B3LYP/6-31+G*//DFT/B3LYP/6-31G* level calculations reproduce three- and

Table 1 Activation energies (kJ mol^{-1}) of benchmark reactions relevant to the present study

	DFT/B3LYP				MP2		
Reaction	6-31G*	6-31+G*	6-311++G**	cc-pVTZ	6-31G*	6-31+G*	Ref.
(4)	230.2	**234.8**	239.0	233.1	*280.7*	273.0	241.3[28]
(5)	187.3	**184.4**	200.8	188.2	*219.3*	212.4	188.3[28]
(6)	326.6	**321.2**	304.3	307.0	*377.5*	372.3	318.4[28]
(7)	329.7	**349.2**	312.2	315.5	*386.0*	382.1	352.5[28]
(8)	241.3	**258.4**	225.6	249.8	*298.0*	289.1	242.6[58]
(9)	88.8	**97.9**	101.6	103.3	*73.8*	76.4	100.8[47]
Max. dev.	22.8	**15.8**	40.3	37.0	*59.1*	53.9	
Av. dev.	9.4	**5.9**	14.5	11.0	*40.9*	35.0	

four-centre HCl elimination barriers from *trans*-$C_2H_2Cl_2$ (reactions (6) and (7)) calculated at the QCISD(T)/6-311+G(d,p)//MP2/6-31G* level of theory[28] very closely, as well as matching the Cl and H migrations of reactions (4) and (5) calculated at the same level of theory. The experimental value for reaction (8), the four-centre elimination of HCl from $C_2H_4Cl_2$, is rather less well reproduced. However, the DFT/B3LYP/6-31G* level results provide a much better estimate; in fact, they reproduce exactly the value measured for reaction (8) by Rajakumar *et al.*[46] who quote 241.8 ± 8.4 kJ mol^{-1}. Also of great importance is reproducing Diels–Alder cycloaddition barriers (reaction (9)), since most adducts considered in the present work are formed *via* steps leading to three-membered rings; there is very good agreement with our results and those determined experimentally,[47] with an activation energy of 100.8 ± 12.9 kJ mol^{-1}. Table 2 lists absolute energy calculations for all ethylene and acetylene reactants involved in our studies, as well as the HCl product.

As very few of the relevant compounds have had the molar absorption coefficients of appropriate vibrational modes determined experimentally, all IR intensities used have been taken from vibrational modes calculated at the same time as geometry optimisations. Modes chosen need to be intense to allow for the detection of low concentrations of a particular species; however, care had to be taken to ensure that these peaks did not overlap with any other species. The vibrations identified are listed in Table 3.

For a number of species (C_2HCl, C_2H_2 and C_4HCl), only the Q-branches of the selected modes are observable. Measurements of the intense bending mode that we have monitored for C_2H_2 (for which we have a pure sample) confirm expectations that the Q-branch area is approximately half of the total area of the rovibrational peaks. We have made the assumption that this approximation is also valid for C_2HCl and C_4HCl; thus, the area utilised in the concentration calculations of these species is double the area of the Q-branch.

Justification for the use of DFT-calculated molar absorption coefficients must come from comparison with experimentally determined values. The limited use of FTIR spectroscopy in product quantification of compounds similar to those we are using means there is very limited experimental data on absorption coefficients. However, as noted in Table 3, measured data of the integrated absorption intensities for *cis*- and *trans*-dichloroethylene are available.[48] Concentrations calculated with the measured values are larger than those calculated with DFT-based absorption intensities; for the *trans*-isomer, approximately 16–19% larger, while for the *cis*-isomer they are approximately 31–38% larger. From this, we conclude that concentration estimates should be reasonable within a factor of two or so; however, there may be more error in the estimate of C_2HCl and C_4HCl due to the previously stated assumption that the Q branch area is approximately half of the total area of a given spectral feature. It must also be noted, however, that species exhibiting high absorbances may no longer follow Beer's law, introducing further error into concentration determinations. It has also been noted by Hall *et al.*[55] that the break-down of Beer's law is very much more pronounced in species, HCl for example, with rotational lines narrower than the resolution of the instrument. They also note that absorbance is very sensitive to the total pressure. These factors lead us to conclude that the concentrations reported represent order-of-magnitude estimates rather than quantitative measurements.

Experimental

trans-Dichloroethylene

The time-resolved yields of major products formed during the laser pyrolysis of 20 Torr of *trans*-$C_2H_2Cl_2$ (in 8 Torr of SF_6)

Table 2 Absolute energies (hartree) of reagent species and HCl at various levels (all calculated using DFT/B3LYP methods)

Species	Label	*E* (6-31G*)	ZPE (6-31G*)	Single-point *E* (6-31+G*)
Chloroethylene	MCE	−538.1853813	0.042821763	−538.1909948
Acetylene	Ace	−77.3256525	0.026648276	−77.3330925
Cis-Dichloroethylene	*cis*-DCE	−997.7786028	0.034285972	−997.7842776
Trans-Dichloroethylene	*trans*-DCE	−997.7783399	0.033960861	−997.7837982
Chloroacetylene	Mca	−536.9132621	0.018829912	−536.9198012
Trichloroethylene	TCE	−1457.365503	0.024773899	−1457.3714429
Dichloroacetylene	Dca	−996.4990427	0.01084489	−996.5046655
HCl	HCl	−460.795512	0.006185876	−460.7978383

Table 3 Position, assignment, and strengths of IR modes used in obtaining the concentration changes

Species	ν/cm^{-1}	Assignment	Strength[a]	Ref.
Trans-$C_2H_2Cl_2$	1201 (s)[b]	B_u ν_{10} C–H Bend	1700 ± 50 L mol^{-1} cm^{-2} (20.38)	49
Cis-$C_2H_2Cl_2$	1303 (m)	B_1 ν_9 C–H Bend	1800 ± 100 L mol^{-1} cm^{-2} (27.69)	49
C_2HCl	604 (s)	π ν_5 C–H Bend	(2 × 45.06)	50
C_2H_2	730.3 (vs)	π_u ν_5 C–H Bend	(2 × 81.06)[c]	51
HCl	~3100–2000 [2944][d]	H–Cl stretch	(9.34)	
C_4HCl	621	π ν_6 C–H Bend	(43.37 + 42.79)[e]	52
1,2,4-$C_6H_3Cl_3$	1035		(62.63)	
C_2HCl_3	783 (s)	a″ ν_{10} C–H out-of-plane bend	(27.86)	53,54
C_4Cl_2	2161 (vs)	Σ_u^+ ν_4 C≡C stretch	(123.62)	55
C_4Cl_4	2216	A C≡C stretch	(162.01)	
1,2,4,5-$C_6H_2Cl_4$	1064		(113.3)	
C_6Cl_6	1344		(188.69 + 189.65)[e]	

[a] Values in parentheses are the IR intensities at the DFT/B3LYP/6-31G* level of theory; in km mol^{-1}. [b] s = strong, m = medium, w = weak, v = very. [c] Total strength of doubly-degenerate mode. [d] Denotes wavenumber of exact vibrational–rotational feature used to calculate area. [e] Loss of symmetry from the ideal leads to two near-degenerate modes and therefore two similar molar absorptivities.

as observed *via* IR spectroscopy are given in Fig. 2. For these observations, the laser power was set to induce the slowest possible reaction consistent with measurable change, so that reaction is likely to be dominated by the route of lowest activation energy. The first product observed was readily identified as *cis*-$C_2H_2Cl_2$; the barrier to isomerization of 228.9 kJ mol^{-1}, as determined experimentally by Jeffers,[56] is much lower than any of the other decomposition or rearrangement steps considered by Riehl *et al.*[28] in their computational study of $C_2H_2Cl_2$ and C_2HCl_3. The initial rate of conversion of the *cis* starting material, together with Jeffers' Arrhenius rate data,[56] provide a very approximate estimate of 800 K for the effective kinetic temperature in the pyrolysis zone of the cell. The next observed product was chloroacetylene, most likely to be the product of the three-centre elimination of HCl (also observed), the second lowest activation energy step as predicted by Riehl *et al.*,[28] at 320.3 kJ mol^{-1} and 318.4 kJ mol^{-1} for *cis*- and *trans*-$C_2H_2Cl_2$, respectively.

The only C_4-species observable by IR spectroscopy was C_4HCl, which began to appear at approximately the same time that the concentration of C_2HCl started to decay significantly. This suggests that C_4HCl formation is mediated by the C_2HCl initial product, and more generally implicates chlorinated acetylenes as intermediates in the formation of diacetylene species. Traces of acetylene, and also of 1,2,4-trichlorobenzene, were also evident. After a period of 10 minutes, the amount of HCl rose to equal that of the starting material, while the carbon-weighted total concentration of IR detectable C-containing species in the gas phase decreased; this was accompanied by visible evidence of solid deposition. At higher laser power, very similar (albeit faster) profiles were obtained, with some indication of the elimination of more than one HCl per starting molecule.

GC-MS investigations, with samples drawn at four representative times over the course of the reaction, revealed a number of additional compounds at concentrations too low to be observed by IR spectroscopy, in particular, diacetylene, trichloroethylene, and a number of $C_4H_2Cl_2$ species (isomers of dichlorovinylacetylene); in much lower concentrations were tetrachloroethylene, other chlorinated analogs of vinylacetylene, $C_4H_{6-x}Cl_x$ species attributed to chlorinated 1,3-butadienes, and chlorinated benzenes. A typical GC trace is shown in Fig. 3. Without calibration standards, accurate quantification is difficult; however, it is reasonable to assume that large differences in peak areas between various compounds correlate to qualitatively similar differences in product

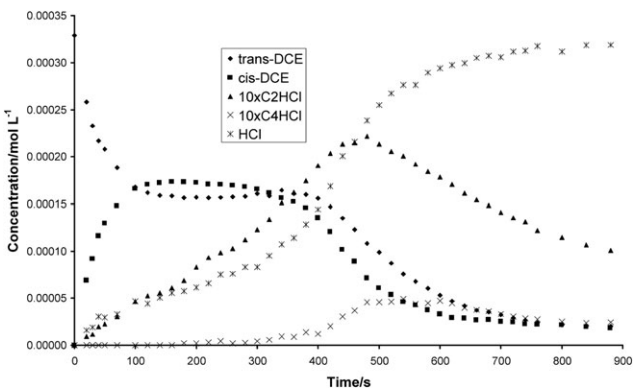

Fig. 2 Time-resolved concentrations of the major *trans*-dichloroethylene laser pyrolysis products.

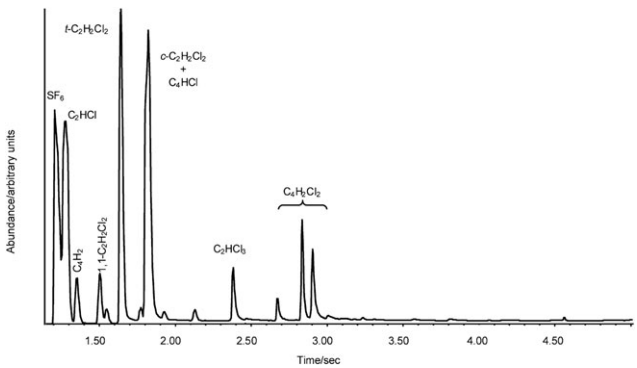

Fig. 3 Representative gas chromatogram of the products of laser pyrolysis of *trans*-dichloroethylene.

concentrations. On this basis, the dichlorovinylacetylenes (with peak areas 100–200 times that of the butadienes) are by far the most abundant C_4 products, second only to chlorodiacetylene (not readily quantifiable from the chromatograms because of exact overlap with the dichloroethylene starting material).

In an attempt to assess the involvement of radical reactions, we have carried out co-pyrolysis studies of 10 Torr of *trans*-$C_2H_2Cl_2$ with 3 Torr of D_2. Even at laser powers set at the threshold for observable reaction, very minor quantities of deuterated products (principally DCl, with lesser amounts of C_2DCl) were observed. This might suggest the production of free radicals (*e.g.*, Cl atoms) that then react with the D_2. However, bimolecular exchange reactions in chlorinated systems such as HCl + D_2 → DCl + HD are fast at the temperatures produced; the activation energy for this reaction has been reported[57] as 238 kJ mol^{-1}, and our own calculations give a value of 260 kJ mol^{-1}. This, followed by back reaction of DCl with acetylenes can easily lead to D incorporation. These results must therefore be regarded as inconclusive.

Trichloroethylene

As above, peak areas of the IR resolvable major products formed during the threshold laser power pyrolysis of 20 Torr C_2HCl_3 were converted to concentrations and plotted as a function of time, and are shown in Fig. 4. Product peaks were found at 706 and 2216 cm^{-1}; the ν_{13} and ν_{18} modes of tetrachlorovinylacetylene (at the MP2/6-31G* level, scaled[58] by 0.9676) were calculated at 669 and 2181 cm^{-1}, in good agreement with those observed. The relative intensities also appeared consistent. Additional peaks were predicted near 840 and 980 cm^{-1}; however, these would be obscured by intense SF_6 features. Minor traces of dichlorodiacetylene were also observed; also noteworthy is a strong peak at 1348 cm^{-1} in the IR spectrum of solid material formed during high reagent pressure pyrolyses, attributed to hexachlorobenzene.

Much more detail became apparent on examination of the partially time-resolved GC-MS data. The major product is dichloroacetylene, not readily observed in the IR since the only IR-allowed transition within our range (the intense ν_3 C–Cl antisymmetric stretch appearing[59] at 993 cm^{-1}) is totally obscured by the SF_6 S–F stretching mode. By analogy with the reactions of dichloroethylene, this is the anticipated major product formed *via* HCl elimination from the parent molecule. No chloroacetylene was observed during our experiments, suggesting that C–Cl homolysis is of little importance.

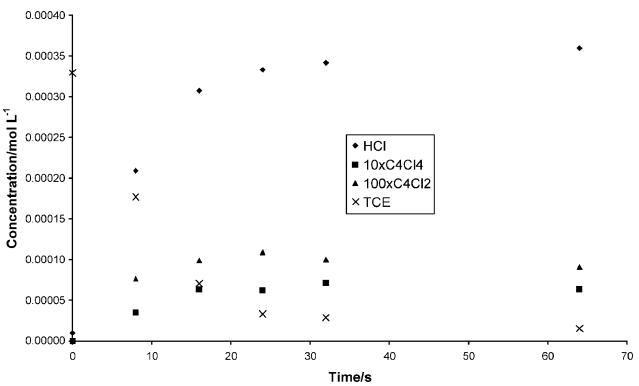

Fig. 4 Time-resolved concentrations of the major trichloroethylene laser pyrolysis products.

Also observed in high yield was tetrachloroethylene; very little hexachlorobenzene was observed in our GC-MS experiments, undoubtedly due to a vapor pressure insufficient for recovery from the gas phase. GC-MS area comparisons confirm the IR spectroscopic data suggesting that C_4Cl_4 is the major product. As minor products, we observe dichlorodiacetylene and hexachloro-1,3-butadiene, and traces of di- and trichlorovinylacetylene and pentachloro-1,3-butadiene.

Acetylene/acetylene reactions: the example of C_2H_2 + C_2HCl

The observations of the previous two sections may be accounted for on the basis of a diacetylene formation mechanism involving the direct reaction of two acetylene species accompanied by HCl elimination. The detailed mechanism of such processes is explored computationally later in this work. The formation of chlorodiacetylene (Fig. 2) after the production of chloroacetylene is readily explained by such a process. Further, the major $C_4H_{2-x}Cl_x$ species observed are also predicted well on the basis of such a mechanism. C_2HCl, the major product in dichloroethylene decomposition, would be expected to lead to C_4HCl + HCl, as observed. The absence of the corresponding product, C_4Cl_2, in trichloroethylene pyrolysis may be directly accounted for by the absence of an HCl elimination step from the proposed intermediate. However, upon co-pyrolysis of an approximately equimolar mixture of $C_2H_2Cl_2$ and C_2HCl_3 in experiments similar to those described above, C_4Cl_2 was formed in much higher yields *via* the analogous proposed reaction (10), which competes with C_2HCl dimerization and lowers the C_4HCl yields:

$$C_2HCl + C_2Cl_2 \rightarrow C_4Cl_2 + HCl \qquad (10)$$

The reaction of chloroacetylene with acetylene would, therefore, be expected to yield C_4H_2 as a major product. To test this hypothesis, chloroacetylene was produced *in situ* by very mild pyrolysis of approximately 20 Torr of *trans*-$C_2H_2Cl_2$; incident laser powers were set such that the higher activation energy C_2H_2 formation route was not significant, thus limiting primary products to C_2HCl exclusively. This was continued until approximately 0.6% (on the basis of background adjusted peak areas) of *trans*-$C_2H_2Cl_2$ remained, at which point observable amounts of the proposed C_2HCl recombination product, C_4HCl, had also started to form (Fig. 5).

The pyrolysis was halted at this stage, and a large overpressure (~60 Torr) of C_2H_2 was added to the pyrolysis cell. Pyrolysis was resumed at a much reduced laser power; this, combined with the high thermal conductivity of a low molecular weight gas like C_2H_2, reduces the effective temperature in the cell considerably below that in the initial stages of $C_2H_2Cl_2$ decomposition. Therefore, any reaction from this point on would have an activation energy no greater, and almost certainly much lower, than the energy required to initiate HCl elimination from $C_2H_2Cl_2$. Partial IR spectra, as a function of time, for these experiments are shown in Fig. 5; it is evident that, in the presence of excess C_2H_2, diacetylene does become the major product, as predicted. These results are

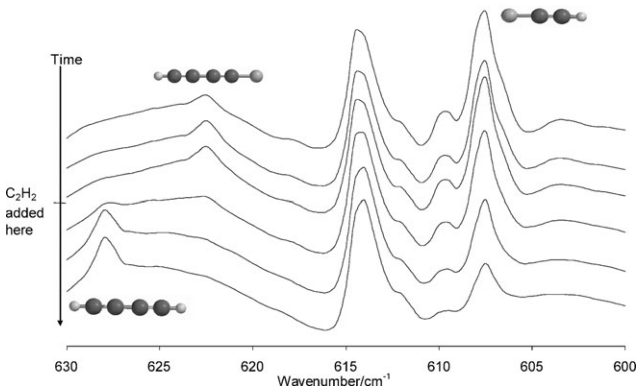

Fig. 5 Acetylenic products C_4H_2, C_4HCl, C_2HCl of *trans*-$C_2H_2Cl_2$ pyrolysis as a function of time; a high pressure of C_2H_2 was added between the third and fourth spectra (absorbance in arbitrary units).

consistent with a $C_4H_{2-x}Cl_x$ formation pathway involving an acetylenic dimer accompanied by HCl elimination, with an activation energy considerably lower than 300 kJ mol^{-1}.

Ethylene/acetylene reactions: the example of $C_2H_2Cl_2$ + C_2H_2

It is not unreasonable, in light of the results above, to anticipate an analogous reaction scheme involving the formation of an ethylene–acetylene adduct, followed by HCl elimination, as a significant mechanism in the formation of chlorinated vinylacetylenes. Again, our observations are consistent with such a mechanism. The results of Fig. 4 shows the immediate formation of perchlorovinylacetylene during trichloroethylene pyrolysis, consistent with rapid consumption of the newly formed C_2Cl_2 by the excess C_2HCl_3 present. Further, the most abundant chlorinated analog of vinylacetylene is as expected in the proposed mechanism; $C_2H_2Cl_2$ and C_2HCl form $C_4H_2Cl_2$, C_2HCl_3 and C_2Cl_2 form C_4Cl_4, and much increased yields of C_4HCl_3 were observed in the $C_2H_2Cl_2$ + C_2HCl_3 co-pyrolyses where the two additional reactions $C_2H_2Cl_2$ + C_2Cl_2 and C_2HCl_3 + C_2HCl are available.

To test such a hypothesis, a co-pyrolysis experiment similar to that described in the previous section was attempted. As before, approximately 20 Torr of reagent, in this experiment *trans*-$C_2H_2Cl_2$, was pyrolysed in an excess (~60 Torr) of acetylene. The expected vinylacetylene species C_4H_3Cl, with four possible isomers, is not readily observed using IR spectroscopy. For this reason, time-resolved GC-MS experiments were the primary means by which the yields of various products were monitored. Laser aperture size and pyrolysis durations were initially chosen such that, in experiments involving 20 Torr of $C_2H_2Cl_2$ alone, only the *cis–trans* isomerization step was accessible. With the higher thermal conductivity of the reacting mixture relative to that observed in the $C_2H_2Cl_2$-only pyrolyses, any reactions subsequently observed must therefore have activation energies much lower than the 320 kJ mol^{-1} required for HCl elimination from $C_2H_2Cl_2$, and also very likely lower than the 228.9 kJ mol^{-1} of the isomerization.[28] The areas of the various chromatographic peaks of interest as a function of time, along with the scaling factors employed, are illustrated in Fig. 6.

Despite the very low temperatures produced in these experiments, a number of reaction products were readily detected. Somewhat surprisingly, high yields of C_2HCl and C_2H_3Cl, together with smaller amounts of 1,1-dichloroethylene, were observed. Of the C_4 products, the major was C_4H_2, followed by C_4H_4 and then the expected C_4H_3Cl; traces of benzene were also formed (not shown in Fig. 6).

Between the second and third pyrolysis, reaction ceased; the generation of light products, such as HCl (which appears in the IR spectra of each sample taken prior to injection into the GC) raises the thermal conductivity, thereby lowering the effective temperature. The production of all compounds ceased at the same point, suggesting a common formation mechanism. This cessation made it necessary to slowly increase the incident laser radiation, achieved through a combination of larger aperture sizes and longer exposure times. During the final pyrolysis, however, gentle reaction was abandoned for a high-temperature reaction aimed at driving product formation to completion. Small amounts of dichlorovinylacetylene were formed; however, the total area of isomers of these compounds is much lower than the total area of C_4H_3Cl isomers (0.3% of the total area of C_4H_3Cl isomers, compared with 4.0% from the pyrolysis of *trans*-$C_2H_2Cl_2$ alone), showing that chlorovinylacetylene is indeed the predominant chlorinated vinylacetylene species, as hypothesized. Small quantities of chlorobenzene and chlorophenylacetylene were observed, with near equal total areas; dichlorobenzene was also present with a total area of approximately half that of C_6H_5Cl and C_8H_5Cl. Very small unquantifiable peaks, with masses and isotope distributions corresponding to $C_{10}H_7Cl$ (very probably chloronaphthalenes) were also detected.

Computational

The experimental results above strongly suggest the existence of low-energy reaction pathways between chlorinated acetylenes + acetylenes and acetylenes + ethylenes. In order to examine more closely the nature of these reactions, we have carried out an extensive series of computational studies of possible routes in these systems. We have attempted to ensure that representative reactions for all potential processes were considered; this search was therefore guided by the early computational work by Hehre and Pople,[60] who considered the relative energies and dipole moments of minima on the C_4H_4 and C_4H_6 PESs. Several of their isomers were not considered in our study due to their lack of structural relationship to the proposed reagents, and the observed predominance of HCl eliminations in the reactions of the chlorinated analogs.

The *cis–trans* isomerization of dichloroethylene (which leads to no complicating subsequent reaction) provides a very convenient internal benchmark. Given the measured activation energy of 229 kJ mol^{-1}, it is unlikely that initiation reactions with activation energies significantly greater than this will play a major role. C–H or C–Cl bond scissions (ranging from 350 to 520 kJ mol^{-1} for sp^3 and sp C, respectively) may therefore be ruled out, and we have concentrated on possible molecular processes.

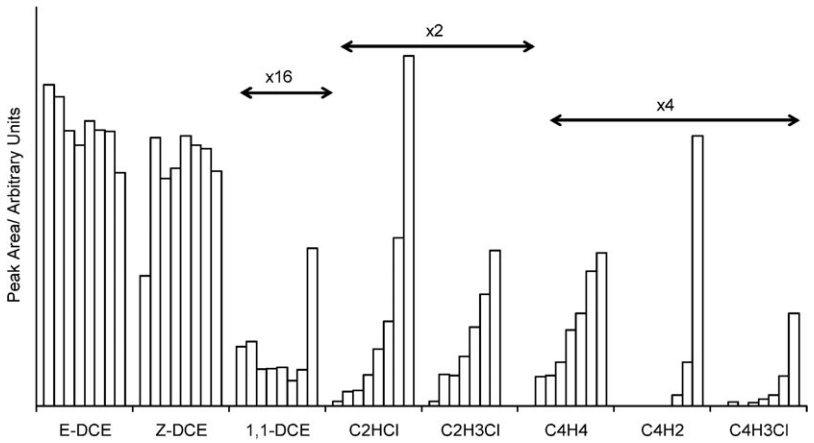

Fig. 6 Chromatographic peak areas of major products observed in the co-pyrolysis of *trans*-$C_2H_2Cl_2$ in excess C_2H_2, as a function of time (time proceeds left to right within each product cluster, approximately 2 min per measurement—see text).

Acetylene–acetylene reactions

There are several conceivable stable products of reaction between two acetylene molecules. Since the pioneering work of Hehre and Pople,[60] the C_4H_4 PES has been thoroughly explored, most recently by Cremer *et al.*[61] At all levels of computation, the relative energies of the stable local minima are similar; those calculated at our chosen DFT/B3LYP/6-31G* level (including zero point vibrational energies) are shown in Fig. 7. The lowest energy forms are the linear vinylacetylene and butatriene, followed by the ring methylenecyclopropene and cyclobutadiene; diacetylene + H_2 has only marginally lower energy than the acetylene reactants, while tetrahedrane lies some 40 kJ mol^{-1} higher. The most significant change on substitution of one or more hydrogens by chlorine appears in the analogous diacetylene + HCl form; largely because of the high HCl bond strength, this form is substantially stabilized. The relative energies for the C_4H_3Cl system (*i.e.*, that relevant to the C_2HCl + C_2H_2 co-pyrolysis experiments described above) are also illustrated in Fig. 7.

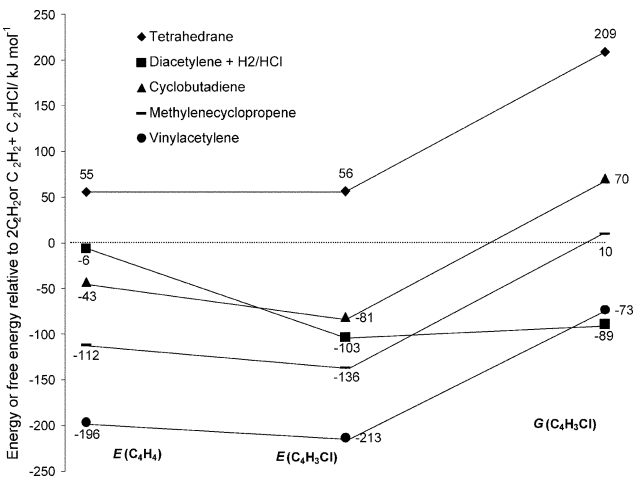

Fig. 7 Calculated energies (kJ mol^{-1}) of local minima on the C_4H_4 and C_4H_3Cl potential energy surfaces, together with free energies for the C_4H_3Cl system. All reported values are relative to the relevant acetylene + acetylene system.

Under pyrolysis conditions, the thermodynamic contributions of translational, rotational and vibrational motion, as well as entropic terms, must also be considered. Of these, entropic terms are more significant; entropies of bimolecular systems are typically some 150 J K^{-1} mol^{-1} greater than those of unimolecular systems of comparable mass, so that at typical pyrolysis temperatures of 1000 K the free energies of the latter are shifted up by about 150 kJ mol^{-1} relative to the former. The results of precise calculations of the free energies of the C_4H_3Cl system at 1000 K including all thermodynamic contributions are also illustrated in Fig. 7. This confirms our expectation that the most stable form on the C_4H_3Cl PES is C_4H_2 + HCl, consistent with our experimental observations. For the C_4H_4 system, however, vinylacetylene remains as the lowest free energy form.

The relative free energies described above, coupled with our experimental observations, strongly suggest that acetylene dimerization together with HCl elimination is a major production route for diacetylenes, along with the potential for such dimerizations to represent competitive pathways to vinylacetylenes. A full series of possible molecular reactions for a number of $C_2H_{2-x}Cl_x$–$C_2H_{2-y}Cl_y$ systems was therefore examined.

We first examined direct molecular routes to the observed end-products, namely chlorovinylacetylene and diacetylene + HCl. It soon became apparent that the presence of the chlorine has a profound effect on the feasibility of such routes. The activation energy of direct molecular addition with the concerted elimination of HCl for the system C_2H_2 + C_2HCl is calculated to be 150 kJ mol^{-1}, a very low energy reaction pathway readily accessible under our chosen reaction conditions. Together with the pre-exponential *A*-factor calculated for this reaction, this leads to an effective pseudo-first order rate constant at 800 K of the order of 10^{-4} s^{-1} for the disappearance of C_2HCl in the presence of excess C_2H_2, entirely consistent with observation. The transition state leading to these products is illustrated in the left hand section of Fig. 8. The corresponding activation energy for C_2HCl + C_2HCl to yield HCl + H–C≡C–C≡C–Cl is even lower at 100 kJ mol^{-1}, consistent with the well known instability of chloroacetylene.

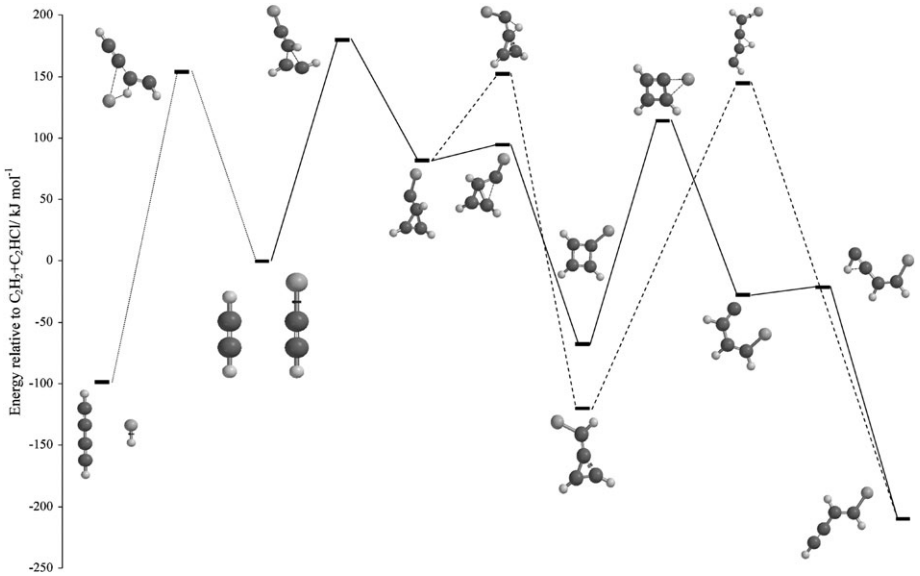

Fig. 8 Intermediates, transition states and energies/kJ mol^{-1} on the C_4H_3Cl potential energy surface, all relative to C_2H_2 + C_2HCl.

We were not able to locate a feasible single-step route to chlorovinylacetylene (by direct insertion of acetylene into a C–Cl bond, for example), and we have therefore ruled out this process as a likely mechanism. As a result, we have explored instead the formation of adducts which might then rearrange to the observed products. The concept of an acetylene–acetylene molecular adduct was first proposed by Benson,[62] who considered a 1,4-biradical, ·CH=CH–CH=CH·, as the key species in vinylacetylene formation. Benson estimated ΔH° for formation of the biradical from $2C_2H_2$ to be 110 kJ mol^{-1}, and thus a feasible step. Attempts to optimize the geometries of chlorinated analogs of Benson's 1,4-biradical resulted in conversion of $C_4H_{4-x}Cl_x$ from a butadiene-like geometry to one of the many carbene species identified in the work of Cremer *et al*.[61] The energy of the resulting adduct for $2C_2H_2$ is 183 kJ mol^{-1} above that of the reactants at our highest level of theory, and hence was not considered to be of practical significance by Cremer *et al* and other workers.[61] However, chlorinated analogs were found to be considerably lower in energy, consistent with the well-known stabilization of carbenes by electron-withdrawing groups; in the C_4H_3Cl system, for example, the three possible isomers lie 158, 120 and 64 kJ mol^{-1} above the reactants. This factor, together with the readily apparent structural relationship of this adduct with both the acetylene + acetylene reactants and possible products such as methylenecyclopropene, led us to consider it as an initial intermediate.

A series of reactions for the most stable initial adduct in the example C_2H_2–C_2HCl system is illustrated in the right hand portion of Fig. 8, showing the geometries and the relative energies of transition states and intermediates on this particular PES. The activation energy for formation of the lowest energy C_4H_3Cl carbene isomer from C_2H_2 + C_2HCl is relatively low at 170 kJ mol^{-1}, rendering this reaction quite feasible under our pyrolysis conditions. It should also be noted that this is considerably more facile than a direct 1,2-shift in either reactant alone to produce a carbene (reactions (4) and (5) of Fig. 1 and Table 1). The frontier orbitals involved in the formation of this initial adduct are illustrated in Fig. 9, and illustrate the very effective interaction between the HOMO and LUMO of the two reactants.

Conversion of this carbene to chloromethylenecyclopropene *via* a 1,2 H-shift is also energetically feasible, with a calculated activation energy of 130 kJ mol^{-1}, as illustrated in Fig. 8. The intermediacy of methylenecyclopropene in the formation of vinylacetylenes has been widely studied, most notably in recent matrix isolation studies of the addition of (usually fluorinated) vinylidene to acetylene.[63–65] Vinylidenes were produced in matrices at approximately 10 K after UV irradiation ($\lambda <$ 248 nm), and upon annealing at 30–40 K underwent rapid addition to residual acetylene molecules to form methylenecyclopropene derivatives. Further irradiation at 420 nm generally resulted in formation of vinylacetylene and butatriene at the expense of methylenecyclopropene. The reaction of difluorovinylidene with acetylene, yielding (difluoromethylene)cyclopropene, followed by irradiation under these conditions, was shown to give 1,1-difluorobut-1-ene-3-yne,[64]

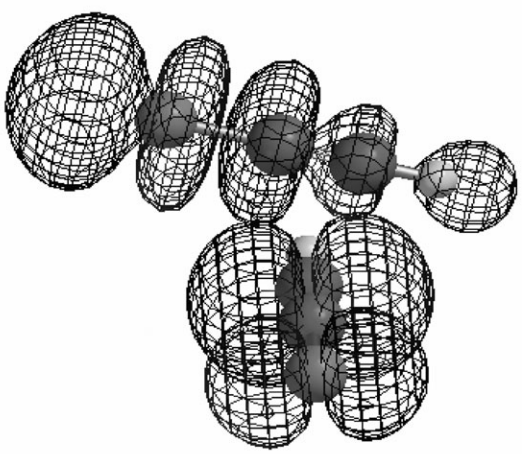

Fig. 9 Frontier orbitals in the formation of the C_2HCl + C_2HCl adduct.

providing clear experimental evidence for the migration of a ring hydrogen in the formation of vinylacetylene, as found in our computational studies.

As also noted in matrix isolation studies, after irradiation at much higher energies (λ = 193 nm), methylenecyclopropene and vinylacetylene yield diacetylene.[65] The higher energies necessary are rationalized by noting that diacetylenes form either by sequential H losses or unimolecular H_2 elimination. However, the relative ease of formation of diacetylene species in our experiments indicates that formation is unlikely to be the result of H atom bond cleavage in the vinylacetylenes. Furthermore, although C–Cl bonds are typically weaker than C–H bonds, the relatively low abundance of C_4Cl_2 during C_2HCl_3 pyrolysis suggests that C–Cl bond cleavages are not responsible either. As discussed above, the dominance of HCl elimination processes suggests that direct molecular reactions are instead the major sources of diacetylenes.

As Fig. 8 indicates, there may also be possible routes involving four-membered rings, cyclobutadienes in this case. Our calculations indicate that this route is competitive with the three-membered ring route, but the experimental observations referred to above lead us to favor the latter.

Acetylene–ethylene reactions

Our experimental evidence suggests that reaction between acetylene and chlorinated ethylenes is even more facile than the acetylene–acetylene case discussed above; reaction between dichloroethylene and acetylene proceeds under very mild conditions where HCl elimination from the dichloroethylene reactant itself does not occur. Calculations similar to those described above indeed show that concerted addition/HCl elimination for this system indeed has a very low activation energy. For the example *cis*-$C_2H_2Cl_2$ + C_2H_2 case, the activation energy is calculated to be 118 kJ mol^{-1}, lower even than the *cis–trans* isomerization, consistent with our observations. On the other hand, the activation energy for formation of the corresponding cyclopropylcarbene adduct is somewhat higher at 210 kJ mol^{-1}, and it is therefore predicted that the formation of the corresponding linear butadienes is considerably less favored. This is entirely consistent with our experimental observations. The energies and geometries of transition states and intermediates involved in the *cis*-$C_2H_2Cl_2$ + C_2H_2 system are illustrated in Fig. 10.

The experiments also provide evidence for relatively low energy HCl transfer reactions between chlorinated ethylenes and acetylenes. The concerted three-centre elimination of HCl from either *cis*- or *trans*-$C_2H_2Cl_2$ and transfer to C_2H_2 is calculated to have an activation energy of 257 kJ mol^{-1}, considerably lower than the 318.4 kJ mol^{-1} for the isolated three-centre loss, and not much greater than the *cis–trans* isomerization activation energy. This accounts for the appearance of C_2HCl (rapidly formed from the chlorovinylidine initial product) and C_2H_3Cl in the C_2H_2 + $C_2H_2Cl_2$ co-pyrolysis studies, leading to an equilibrium mixture of isomers. The 1,1-dichloroethylene observed is readily produced in a reverse HCl transfer reaction. The wide range of C_4 products observed then arises from subsequent acetylene–ethylene/HCl loss reactions among the various possible combinations.

Ethylene–ethylene reactions

It is natural to enquire whether direct ethylene–ethylene dimerization accompanied by HCl elimination similar to the reactions described for acetylenes in the two previous sections might occur. Our experimental results suggest that this is not a significant route, since we observe very little of the chlorinated butadiene products expected from this process. Our calculations support this conclusion, as we have been unable to locate transition states involving HCl elimination accompanied by direct reaction between chlorinated ethylenes. The one such system where this process does appear to occur is the intramolecular 1,6-elimination of HCl and ring closure in 1-chlorohexa-1,3,5-triene, where the activation energy is calculated to be only 35 kJ mol^{-1}. This is entirely consistent with the observed thermal instability of this compound; the one report of its synthesis notes that it decomposes above −20 °C with the

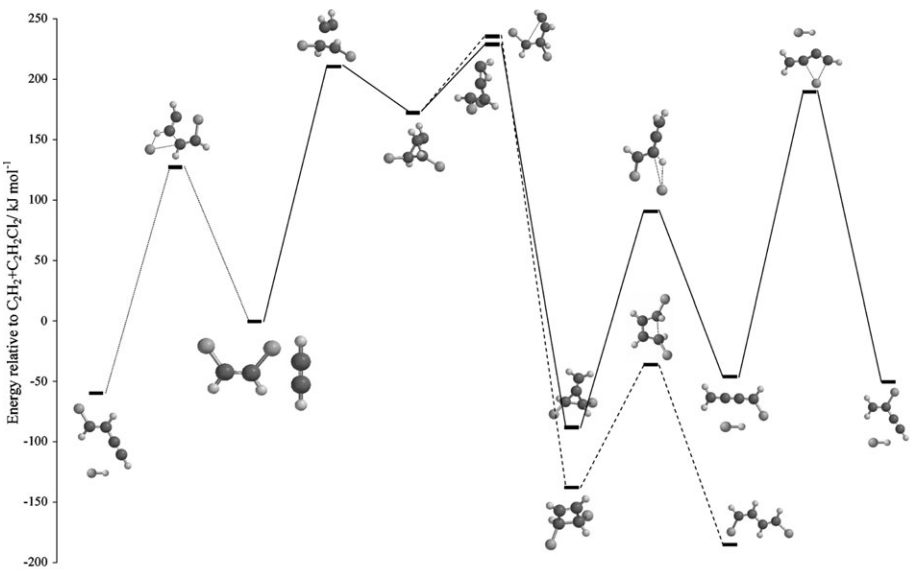

Fig. 10 Intermediates, transition states and energies/kJ mol^{-1} on the $C_4H_4Cl_2$ potential energy surface, all relative to *cis*-$C_2H_2Cl_2$ + C_2H_2.

elimination of HCl (the second product was not identified, but was presumably benzene).[66]

Conclusions

In experimental studies of pyrolytic reactions of chloroethylenes at temperatures too low to involve free radicals, we have found that chlorinated vinylacetylenes are readily formed. The major observed vinylacetylenes in each case are consistent with direct reaction of the parent ethylene and the relevant acetylene formed from the ethylene accompanied by HCl elimination, or with dimerization and reaction of these acetylenes. The competing acetylene–acetylene reactions explain the observed high yields of the dominant chlorinated diacetylene, and the lower than anticipated C_4Cl_2 yields observed in the C_2HCl_3 pyrolysis system. Co-pyrolyses of various ethylene-acetylene mixtures are also accommodated in a molecule-molecule reaction model. Intermediates in the previously studied radical–molecule[1,2,11–14,24–27,67,68] processes may not be formed as rapidly as previously assumed, at least for the C_2HCl_3 system, on the basis of the short lifetimes of vinyl radicals[69,70] previously presumed to propagate such reactions. Matrix isolation experiments have shown that the vinylidene–acetylene recombination[63–65] product, also favored by many as the predominant route in vinylacetylene formation,[15,22] is not present unless high yields of vinylidene are produced *via* photolytic means.[71]

Computational investigations using density functional theory of novel molecular reactions between chlorinated ethylenes and acetylenes have confirmed the feasibility of direct bimolecular reaction accompanied by HCl transfer or elimination. They also show that cyclizations may occur between an acetylenic carbon and the two carbons of a second acetylene or ethylene reactant, forming a strained cyclopropane or cyclopropene carbene. The activation energies of both formation processes are much lower than either the HCl elimination or C–Cl bond cleavages proposed to initiate ethylene decomposition. Rapid three-centre HCl elimination from the initial carbene adducts results in the ready formation of methylenecyclopropenes or methylenecyclopropanes. These are relatively stable intermediates in the sense they are likely to be trappable in low-temperature matrices, but are likely to convert rapidly to vinylacetylenes or butadienes during pyrolysis.

With the completion of the computational study, we have identified the likely trappable intermediates in proposed molecule–molecule reactions of chlorinated ethylenes and acetylenes. Future work will involve matrix isolation-IR spectroscopic investigations, supplemented by matrix isolation-EPR studies, to search for the methylenecyclopropenes, cyclobutadienes, and vinyl radicals involved in the formation of C_4 products at various temperatures in an attempt to better understand molecular growth processes in high temperature environments. We shall also investigate the growth of larger products, particularly ring-based systems.

Acknowledgements

The authors thank the University of Auckland, the Marsden Fund and Lottery Science for grants towards equipment. We also gratefully acknowledge the University of Auckland for financial support of Grant McIntosh through a Guaranteed Doctoral Scholarship.

References

1 X. Xu and P. D. Pacey, *Phys. Chem. Chem. Phys.*, 2001, **3**, 2836.
2 T. Tanzawa and W. C. Gardiner, Jr, *J. Phys. Chem.*, 1980, **84**, 236.
3 X. Xu and P. D. Pacey, *Phys. Chem. Chem. Phys.*, 2005, **7**, 326.
4 E. F. Greene, R. L. Taylor and W. L. Patterson, *J. Phys. Chem.*, 1958, **62**, 238.
5 H. Ogura, *Bull. Chem. Soc. Jpn.*, 1977, **50**, 1044.
6 C. H. Wu, H. J. Singh and R. D. Kern, *Int. J. Chem. Kinet.*, 1987, **19**, 975.
7 K. H. Homann and H. G. Wagner, *Eleventh Symposium [International] on Combustion*, The Combustion Institute, Pittsburgh, PA, 1967, p. 371.
8 M. Ehbrecht, M. Faerber, F. Rohmund, V. V. Smirnov, K. Stelmakh and F. Huisken, *Chem. Phys. Lett.*, 1993, **214**, 34.
9 Y. Chen, H. Zhang, Y. Zhu, D. Yu, Z. Tang, Y. He and C. Wu Wang, *Mater. Sci. Eng., B*, 2002, **95**, 29.
10 H. Richter, E. De Hoffmann, R. Doome, A. Fonseca, J.-M. Gilles, J. B. Nagy, P. A. Thiry, J. Vandooren and P. J. van Tiggelen, *Carbon*, 1996, **34**, 797.
11 R. N. Pease, *J. Am. Chem. Soc.*, 1929, **51**, 3470.
12 C. G. Silcocks, *Proc. R. Soc. London, Ser. A*, 1957, **242**, 411.
13 G. J. Minkoff, D. M. Newitt and P. Rutledge, *J. Appl. Chem.*, 1957, **7**, 406.
14 M. H. Back, *Can. J. Chem.*, 1971, **49**, 2199.
15 R. P. Durán, V. T. Amorebieta and A. J. Colussi, *J. Phys. Chem.*, 1988, **92**, 636.
16 G. J. Minkoff, *Can. J. Chem.*, 1958, **36**, 131.
17 M. Ahmed, D. S. Peterka and A. G. Suits, *J. Chem. Phys.*, 1999, **11**, 4248.
18 C. D. Sherrill, *J. Chem. Phys.*, 2000, **113**, 1447.
19 I. D. Gay, G. B. Kistiakowsky, J. V. Michael and H. Niki, *J. Chem. Phys.*, 1965, **43**, 1720.
20 J.-F. Riehl and K. Morokuma, *J. Chem. Phys.*, 1994, **100**, 8976.
21 E. Ghibaudi and A. J. Colussi, *J. Phys. Chem.*, 1988, **92**, 5839.
22 J. H. Kiefer and W. A. von Drasek, *Int. J. Chem. Kinet.*, 1990, **22**, 747.
23 J. H. Kiefer, *Int. J. Chem. Kinet.*, 1993, **25**, 215.
24 P. H. Taylor, D. A. Tirey, W. A. Rubey and B. Dellinger, *Combust. Sci. Technol.*, 1994, **101**, 75.
25 B. L. Earl and R. L. Titus, *Collect. Czech. Chem. Commun.*, 1995, **60**, 104.
26 D. Drijvers, R. De Baets, A. De Visscher and H. Van Langenhove, *Ultrason. Sonochem.*, 1996, **3**, S83.
27 C. F. Cullis, G. J. Minkoff and M. A. Nettleton, *Trans. Faraday Soc.*, 1962, **58**, 1117.
28 J.-F. Riehl, D. G. Musaev and K. Morokuma, *J. Chem. Phys.*, 1994, **101**, 5942.
29 J. Levin, H. Feldman, A. Baer, D. Ben-Hamu, O. Heber, D. Zajfman and Z. Vager, *Phys. Rev. Lett.*, 1998, **81**, 3347.
30 R. Schork and H. Köppel, *Chem. Phys. Lett.*, 2000, **326**, 277.
31 W. M. Shaub and S. H. Bauer, *Int. J. Chem. Kinet.*, 1975, **7**, 509.
32 J. Pola, *Collect. Czech. Chem. Commun.*, 1981, **46**, 2854.
33 G. A. Atiya, A. S. Grady, S. A. Jackson, N. Parker and D. K. Russell, *J. Organomet. Chem.*, 1989, **260**, 180.
34 D. K. Russell, *Chem. Soc. Rev.*, 1990, **19**, 407.
35 J. L. Lyman, *J. Chem. Phys.*, 1977, **67**, 1868.
36 S. Davison and M. Barton, *J. Am. Chem. Soc.*, 1952, **74**, 2307.
37 G. H. Miller and E. W. R. Steacie, *J. Am. Chem. Soc.*, 1958, **80**, 6486.
38 R. R. Baldwin, R. W. Walker and D. H. Langford, *Trans. Faraday Soc.*, 1969, **65**, 2116.
39 N. R. Hore and D. K. Russell, *New J. Chem.*, 2004, **28**, 606.
40 C. Lee, W. Yang and R. G. Parr, *Phys. Rev. B: Condens. Matter*, 1988, **37**, 785.
41 A. D. Becke, *J. Chem. Phys.*, 1993, **98**, 5648.
42 A. P. Scott and L. Radom, *J. Phys. Chem.*, 1996, **100**, 16502.
43 G. R. Allen and D. K. Russell, *New J. Chem.*, 2004, **28**, 1107.

44 J. D. Ferguson, N. L. Johnson, P. M. Kekenes-Huskey, W. C. Everett, G. L. Heard, D. W. Setser and B. E. Holmos, *J. Phys. Chem. A*, 2005, **109**, 4540.
45 B. Rajakumar and E. Arunan, *Phys. Chem. Chem. Phys.*, 2003, **5**, 3897.
46 B. Rajakumar, K. P. J. Reddy and E. Arunan, *J. Phys. Chem. A*, 2002, **106**, 8366.
47 V. D. Knyazev, *J. Phys. Chem. A*, 2004, **108**, 10714.
48 K. Tanabe and S. Saeki, *Bull. Chem. Soc. Jpn.*, 1974, **47**, 2545.
49 L. Zhu and J. W. Bozzelli, *Chem. Phys. Lett.*, 2002, **362**, 445.
50 T. Shimanouchi, *Tables of Molecular Vibrational Frequencies Consolidated Volume I*, National Bureau of Standards, Washington, DC, 1972.
51 P. Klaeboe, E. Kloster-Jensen and S. J. Cyvin, *Spectrochim. Acta, Part. A*, 1967, **23**, 2733.
52 Y. Jugnet, J. C. Bertolini, L. A. M. M. Barbosa and P. Sautet, *Surf. Sci.*, 2002, **505**, 153.
53 T. J. Houser, R. B. Bernstein, R. G. Miekka and J. C. Angus, *J. Am. Chem. Soc.*, 1955, **77**, 6201.
54 P. Klaboe, E. Kloster-Jensen, E. Bjarnov, D. H. Christensen and O. F. Nielsen, *Spectrochim. Acta, Part A*, 1975, **31**, 931.
55 M. J. Hall, D. Lucas and C. P. Koshland, *Environ. Sci. Technol.*, 1991, **25**, 260.
56 P. M. Jeffers, *J. Phys. Chem.*, 1972, **76**, 2829.
57 H. Steiner and E. K. Rideal, *Proc. R. Soc. London, Ser. A*, 1939, **173**, 503.
58 J. A. Seetula, *J. Chem. Soc., Faraday Trans.*, 1998, **94**, 1933.
59 D. McNaughton, *Struct. Chem.*, 1992, **3**, 245.
60 W. J. Hehre and J. A. Pople, *J. Am. Chem. Soc.*, 1975, **97**, 6941.
61 D. Cremer, E. Kraka, H. Joo, J. A. Stearnsyc and T. S. Zwier, *Phys. Chem. Chem. Phys.*, 2006, **8**, 5304.
62 S. W. Benson, *Int. J. Chem. Kinet.*, 1989, **21**, 233.
63 W. Sander and C. Kötting, *Chem.–Eur. J.*, 1999, **5**, 24.
64 C. Kötting, W. Sander and M. Senzlober, *Chem.–Eur. J.*, 1998, **4**, 2360.
65 R. Wrobel, W. Sander, D. Cremer and E. Kraka, *J. Phys. Chem. A*, 2000, **104**, 3819.
66 C. W. Spangler and G. F. Woods, *J. Org. Chem.*, 1965, **30**, 2218.
67 M. A. Weissman and S. W. Benson, *J. Phys. Chem.*, 1988, **92**, 4080.
68 P. H. Taylor, D. A. Tirey and B. Dellinger, *Combust. Flame*, 1996, **104**, 260.
69 M. G. Bryukov, S. A. Kostina and V. D. Knyazev, *J. Phys. Chem. A*, 2003, **107**, 6574.
70 Y.-P. G. Wu and Y.-F. Lin, *Combust. Flame*, 2004, **137**, 376.
71 G. Maier and C. Lautz, *Eur. J. Org. Chem.*, 1998, **199**, 769.

